ELSEVIER

Materials Science and Engineering B102 (2003) 2–7

MATERIALS SCIENCE & ENGINEERING B

www.elsevier.com/locate/mseb

Positron beam analysis of structurally ordered porosity in mesoporous silica thin films

A. van Veen [a,*], R. Escobar Galindo [a], H. Schut [a], S.W.H. Eijt [a], C.V. Falub [a], A.R. Balkenende [b], F.K. de Theije [b]

[a] *Defects in Materials, Interfaculty Reactor Institute, Delft University of Technology, Mekelweg 15, NL-2629 JB Delft, The Netherlands*
[b] *Philips Research Laboratories, Prof. Holstlaan 4, NL-5656 AA, Eindhoven, The Netherlands*

Abstract

Positron beam techniques have been employed to characterise low-k dielectric silica based films, which have two or three dimensional structures of nanometre size pores. Pore fractions vary from 5 to 50%. Positrons implanted in the layer slow down and eventually annihilate with the electrons from the layer. However, in pores of the dielectric films positronium (Ps) is formed before annihilation takes place. The two states of Ps (*para*-positronium (p-Ps) and *ortho*-positronium (o-Ps)) are formed with rather different life times of 125 ps and 142 ns, respectively. The behaviour of Ps in the porous material can be described as hot particles with 1 eV initial kinetic energy, which lose their energy by frequent collisions with the atoms of the pore walls. When the pores are interconnected or separated by thin walls allowing permeation of the Ps some of the Ps will effuse from the film into the vacuum. The 2D-ACAR technique enables one to monitor the velocity distribution of the annihilating p-Ps and shows an increasing fraction of surface emitted p-Ps when positrons are implanted closer to the film surface. Measurements of Doppler broadening of 2-gamma annihilation and detection of 3-gamma events (o-Ps) give insight into the frequency of other annihilation events. Combining the results, a complete picture can be obtained of the interactions and transport of the Ps particles in the material. By modelling the Ps behaviour information is obtained on structural parameters of the porous material. A transport model based on multi energy group diffusion of particles describes the results well.

Keywords: Positrons; Positronium; Annihilation; Silica; Pores and percolation phenomena

1. Introduction

Materials with a low dielectric constant ($k < 2.2$) are required for future generations of ICs, in order to substitute the present dielectric layers in ultra large scale integrated (ULSI) devices. Candidates include, e.g. organic and inorganic polymers, and nanoporous silica. A high porosity of the material is necessary to lower the dielectric constant sufficiently. Furthermore, pore sizes should be small (typically < 5 nm). Characterisation of the porous structure by a number of positron annihilation techniques [1–4] has shown to be successful. The majority of positrons after implantation in the material form positronium (Ps) in the pores. Since Ps can be considered as a very light tracer 'atom' with the physical size of a hydrogen atom wandering around in the pore structure it can give information on pore size and transport of gas through the porous structure. In this study the emphasis will be on a description of the Ps history in low-k thin films with well-defined pores. The experimental methods are depth selective Doppler broadening and high resolution 2D-ACAR which measure momentum distributions of annihilating electron–positron pairs and Ps in the films. A companion article describes low-k films in which the composition of the internal surface is modified [5].

2. Sample preparation and experimental procedure

The mesoporous silica samples were produced using solutions containing silicon alkoxides (tetraethylorthosilicate, TEOS) and a surfactant (cetyltrimethylammo-

* Corresponding author. Tel.: +31-15-278-2801; fax: +31-15-278-6422.
E-mail address: avveen@iri.tudelft.nl (A. van Veen).

0921-5107/03/$ - see front matter
doi:10.1016/S0921-5107(02)00752-3

nium bromide, CTAB) or Pluronic F127 (ethylene oxide)$_{106}$(propylene oxide)$_{70}$(ethylene oxide)$_{106}$. During coating deposition the solvents evaporate, micelles are formed and the silicon alkoxide condenses to form (organically modified) silica around the micelles. A well-ordered pore structure is obtained once the micelles are removed from the coating. The TEOS/CTAB system forms at high porosity a three dimensional (3D) hexagonal phase, while the TEOS/F127 system results at high porosity in a two dimensional (2D) hexagonal packing of cylinders in the plane of the surface. The six samples used in this study are all hydrophilic due to the presence of silanol groups at the internal pore surfaces. The film properties are given in Table 1.

The PBA experiments were performed with the positron beams at the Delft Positron Centre [6,7]. The positrons were injected in the samples with energies tuned between 100 eV and 30 keV. The maximum implantation energy corresponds to a typical implantation depth of $\sim$2μm in ceramics of density 2.5 g cm^{-3}. All experiments were carried out at room temperature under a vacuum of about 10^{-6} Pa. The PBA results are described in terms of three parameters (S, W and f-Ps) [8]. The S parameter indicates the fraction of positrons that annihilates with low momentum electrons (valence or conduction electrons). This parameter is related to the open volume defects present in the sample (e.g. pores). The W parameter indicates the fraction of positrons that annihilates with high momentum electrons (core electrons). This parameter is related to the chemical environment where the annihilation takes place. Both parameters can be combined in S–W maps where the different annihilation sites (layers) can be distinguished. The data was analysed with the VEPFIT [7] program. The third parameter (f-Ps) represents the fraction of implanted positrons that is related to *ortho*-positronium (o-Ps) self-annihilation and is observed by 3-γ annihilation. In the companion article the branching of the positrons into different states is presented [5]. For low-k coatings five annihilation states can be distinguished: *para*-positronium (p-Ps), o-Ps annihilation via the pore wall, o-Ps self-annihilation, positron annihilation inside the walls separating the pores, and the fraction of Ps that escapes from the film. The fraction f-Ps is defined such that for highly porous material with large pores f-Ps = 100%.

The 2D-ACAR method [9] measures the deviation from collinearity between the two annihilation photons. This deviation is of the order of a few milliradians. A high-intensity (10^8 e$^+$ s^{-1}) tuneable keV positron beam POSH enables depth-selective studies in the (sub)-micrometer range. 2D-ACAR is measuring exclusively 2-γ annihilation events and is able to resolving p-Ps annihilation and to derive the momentum distribution of the annihilating p-Ps.

3. Results

In Fig. 1 the measured values of S, W, and f-Ps are plotted versus the positron energy for the six samples. In the fourth panel the S–W values are plotted in a so called S–W map. The results are typical for a thin film on a silicon substrate. Positrons entering with a low energy are implanted very shallowly and probe the outer surface and, therefore, yield different S, W parameters than those in the energy range 1–4 keV corresponding to implantation within the films. For energies larger than 4 keV a gradual transition takes place to annihilation in the substrate. Fitting procedures (VEPFIT [6]) have been applied to determine the thickness (by weight) of the film. This thickness agrees well with the weight thickness derived from Table 1 (using thickness and density). Characteristic values derived for S and W of all the films are given in Table 1. They are also indicated in the S–W map of Fig. 2 for six of the films. The Ps fraction varies from very low to about 50% for the investigated hydrophilic samples. Results of hydrophobic films in [5] show even higher values of 85%. In general, the Ps fraction increases with porosity but the fraction is much higher for the high porosity F127 two dimensional structure with large diameter cylinders than for the CTAB three dimensional structure with small diameter pores.

A typical result obtained with the 2D-ACAR setup for the F127 (2c) film is shown in Fig. 2. The momentum

Table 1
Description of the low-k films and measured positron annihilation parameters

Number	Description	Thickness (nm)	Porosity (%)	Pore size (nm)	Density (g cm^{-3})	$S_{\text{rel. layer}}$	$W_{\text{rel. layer}}$	f_{Ps}
1a	TEOS/CTAB 0.01 [a] R[b]	184	10.9	1 (0.5)	2.0	0.954	1.64	0
1b	TEOS/CTAB 0.05 R	267	31.0	1 (0.5)	1.5	0.992	1.46	0.12
1c	TEOS/CTAB 0.1 3D	338	46.3	1.75 (0.25)	1.2	1.010	1.40	0.12
2a	TEOS/ F127 0.0005 R	190	7.4	1 (0.5)	2.0	0.982	1.56	0
2b	TEOS/ F127 0.002 R	285	35.0	1 (0.5)	1.4	0.994	1.40	0.08
2c	TEOS/ F127 0.005 2D	457	44.7	4.5 (0.5)	1.2	0.994	1.48	0.48

[a] Composition ratio.
[b] Ordering: R, random; 2D, two dimensional; 3D, three dimensional.

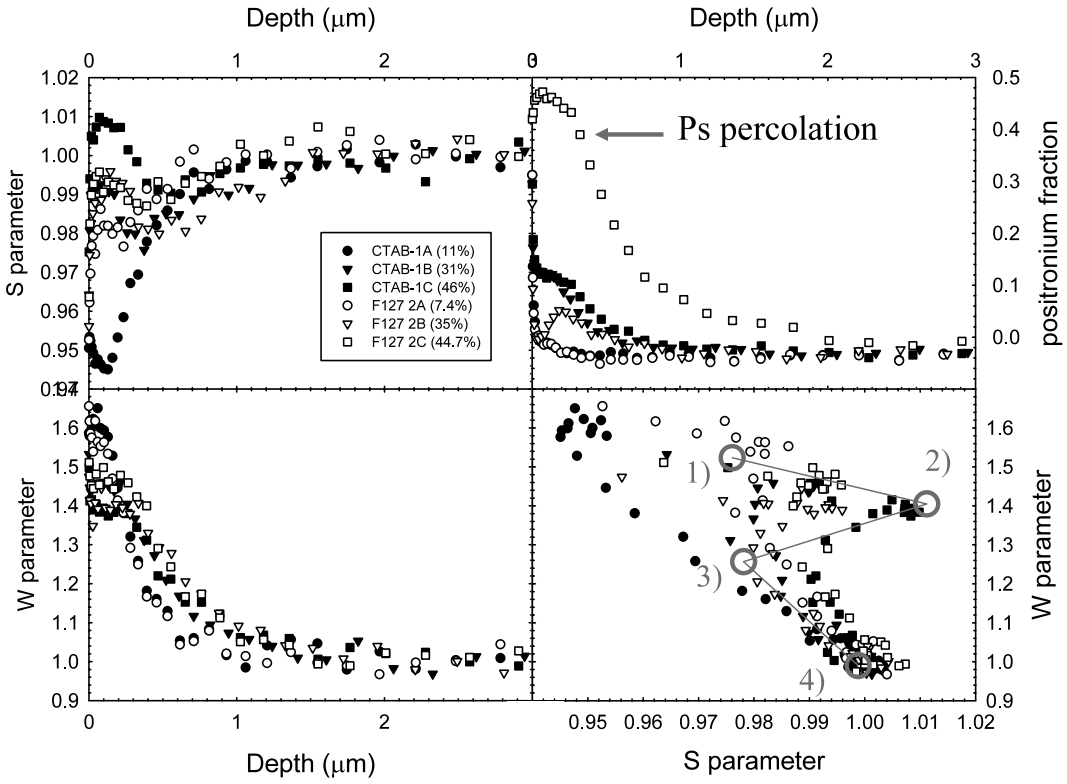

Fig. 1. Positron annihilation parameters S, W, and f-Ps plotted as a function of the average positron implantation depth, and an S, W map showing all the S, W data. For the CTAB-1c film the characteristic annihilation states are given: (1) surface, (2) porous film, (3) interface and (4) Si-substrate.

distribution of the film implanted with 3.5 keV positrons shown in Fig. 2a reveals asymmetry in the y-direction (corresponding to the direction outward directed from the surface). Apparently, the distribution is composed of an isotropic and an anisotropic component. It appears that the latter component is a cosine momentum distribution (Fig. 2b) which can be assigned to p-Ps particles flying off the surface, like a gas molecule effusing from a hole in a volume containing a low density Knudsen gas. The isotropic contribution can be decomposed into a narrow and a broad component. The narrow component can be assigned to p-Ps 'gas' that annihilates inside the pores. In Fig. 3 cross-sections of the momentum distribution in x and y direction are displayed for the film. Analysis of the momentum distribution shows that the average energy of the Ps amounts to 0.9 eV for shallowly implanted and to 0.5 eV for 3.5 keV implanted positrons. An average momentum

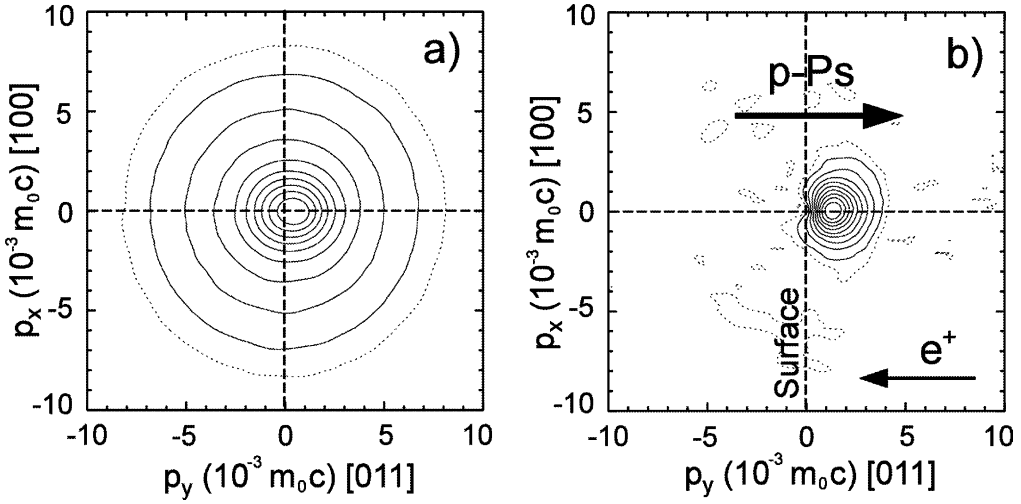

Fig. 2. Momentum distributions measured for sample 127 2c.

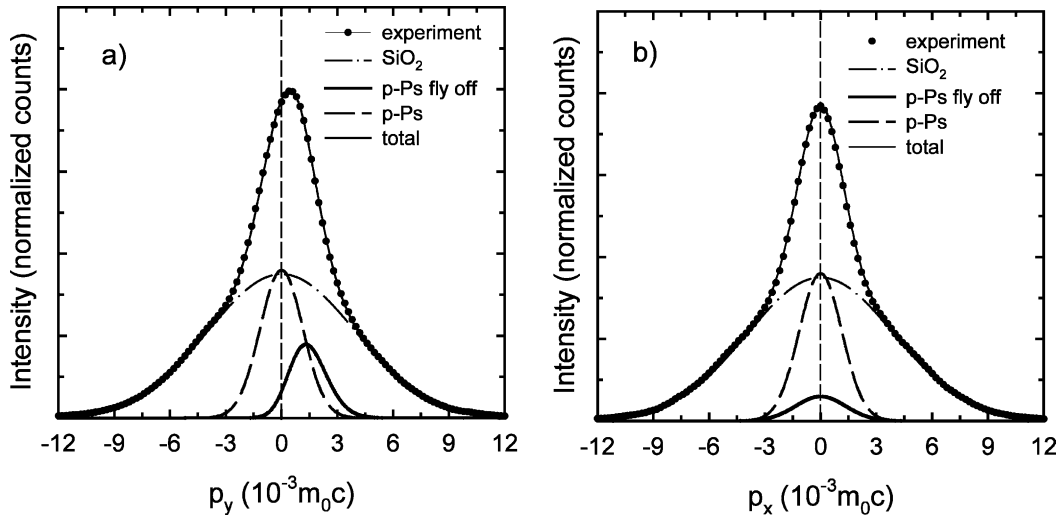

Fig. 3. Cross-sections through momentum distribution measured by 2D-ACAR. (a) Momentum perpendicular to the surface, (b) momentum parallel to the surface.

of 10^{-3} $m_o c$ corresponds to an average Ps kinetic energy of 0.128 eV.

4. Positronium slowing down and transport in porous SiO_2

The implantation profile of positrons can be described by the so called Makhov profile (a derivative of a Gaussian) which is also used for solids without pores [8]. The porosity is taken into account by using the reduced density of the porous silica in the Makhov expression. Positrons do not slow down in the pores, only in the wall material. Ps is formed by combining one of the electrons produced in the track of the slowing down positron with the thermalised positron. The Ps particle is attracted by the pores and is created with a kinetic energy of about 1 eV, as follows from Ps surface emission of Ps from silica and from ACAR measurements on Ps in xerogel [10]. Once Ps is formed, with the two states *p*-Ps and *o*-Ps in a ratio of 1–3, it will behave as an atom in a Knudsen gas. There are only interactions with the walls of the structure but not with other Ps. The reason for this is the short lifetime of Ps average lifetimes for self-annihilation are 125 ps for the *p*-Ps and 140 ns for *o*-Ps, respectively, when self-annihilation occurs. The annihilation of *p*-Ps yields two γ-rays of about 511 keV, the self annihilation of *o*-Ps yields three γ-rays in the energy region 0–511 keV. Annihilation of *o*-Ps is accelerated by a pick-off reaction with the walls of the pores; subsequently, annihilation by two γ-rays occurs.

The transport and cooling of the Ps can be described by approximating the Ps transport by diffusion theory. Let $c(E, x, t)$ be the concentration of Ps at depth x with energy E at time t.

A balance equation can then be written as follows:

$$\frac{\mathrm{d}c(x,\ E)}{\mathrm{d}t} = \frac{D(E)\mathrm{d}^2c(x,\ E)}{\mathrm{d}x^2} - \frac{1}{4}\left(\frac{1}{V}\right)v(E)f_s Oc(x,\ E) + \frac{1}{4} \times \left(\frac{1}{V}\right)v(E'')f_s Oc(x,\ E) + I(x) - \lambda_{\mathrm{Ps}}c(x,\ E) - \frac{\delta r}{r}\ \lambda_{\text{pick-off}}c(x,\ E)$$

where the first term at the right hand side describes the loss/gain by diffusion (the diffusion coefficient D is E dependent), the second term the loss rate by scattering ($E \rightarrow E'$), with final energy $E' = E/\alpha$ after one collision, and the third term the growth rate by scattering ($E'' \rightarrow E$) with energy $E'' = \alpha E$ after one collision.

In a collision with atoms in thermal motion also some energy will be transferred from the atom to the Ps; finally, this will lead to thermalisation of the Ps. This is not yet included in the theory. The fourth term is the implantation rate which is zero for $E < E_0$, the fifth term is the self annihilation rate and the sixth term the pick-off rate (important only for *o*-Ps), with δr the pick-off layer in the pores with radius r.

The diffusion coefficient can be described by $D(E) = 1/6\lambda^2 v$ for 3D ordered and $1/4\lambda^2 v$ for 2D ordered pore structures, where λ is the jump distance = distance between the two centres of neighbouring cavities = $2r + l_w$, with l_w the thickness of the wall separating the pores. V is the attempt frequency, in all directions, of one Ps present in a cavity volume $V = 4/3\pi r^3$, where V1/4 $(1/V)v_{\mathrm{Ps}} f_{\mathrm{O}} O$ where v_{Ps} is the velocity of the Ps derived

from the energy E, $v_{Ps} = V2eE/m_{Ps}$, and f_O is the fraction of Ps that is penetrating through the walls of the cavity given by $f_O = O^*/O$, O^* is the open or transparent part of the wall, f_s is the fraction that scatters off the wall. The factor $1/\alpha$ is close to unity because m_{Ps} is much smaller than the mass of the wall atoms. Its lowest value for maximum energy transfer, is $1/\alpha = (1-m_{Ps}/m_{at})^2/(1+m_{Ps}/m_{at})^2 \sim (1-4m_{Ps}/m_{at})$. The energy loss for Ps with energy E during time Δt equals $1/4(1/V)v(E)\, f_s O$ (collision frequency) $\times \Delta t \times E/\alpha$

The boundary conditions are given by reflection of Ps at the silicon substrate interface at $x = l$: $(dc/dx)_{x=1} = 0$. It is assumed that Ps at the vacuum side is emitted into the vacuum: $c_{(x=0)} = 0$. The emission rate is given by $D(dc/dx)$. The time dependent transport equation is solved numerically.

5. Discussion

The above model applied to an ordered 2D pore structure (e.g. 127 2c) yields a wall thickness of 1.8 nm. The effective p-Ps diffusivity is calculated to be 2 cm^2 s^{-1}, and the diffusion length is 158 nm if the pore transparency parameter $f_O = 0.2$ is taken. It follows from the value of the diffusion length (of the same order as the film thickness) that a significant amount of p-Ps created throughout the film will escape from the surface during its limited lifetime. In [5] it is found that for a sample porosity $> 45\%$, p-Ps effusion is observed. It is very likely that when walls get thinner, i.e. a few times the structural pore size in silica, Ps, which has an effective, quantum mechanically determined, size of about 0.8 nm when it is in interaction with the silica structure, will easily permeate. Numerical results of transport of p-Ps implanted in such a porous film are given in Fig. 4. Time dependent energy distributions of p-Ps at a depth of 200 nm are plotted which show the evolution of the energy from 1 eV at $t = 0$ to a broad stationary energy distribution when equilibrium is established between the implantation of positrons and the annihilation of p-Ps (average life time 125 ps). The bottom figure shows the stationary energy distributions at varying depth. Average energies are 0.35 eV for the deep layers and 0.41 eV for the shallow layers. The energy distributions deviate from the Maxwell–Boltzmann distribution which applies for particles in thermal equilibrium. An important reason is that at any time hot Ps is introduced into the film. It seems that the energy distributions can be described rather well by the sum of two Maxwell–Boltzmann distributions, e.g. one with $kT_1 = 0.11$ eV, and $kT_2 = 0.6$ eV for the distribution with an average energy of 0.35 eV (not shown here).

The above model can be applied and used to fit the measured energy and velocity distributions, together with the other parameters measured in the positron beam experiments. The model will yield fractions for all annihilating modes which contribute to the S and W parameters and the Ps fraction.

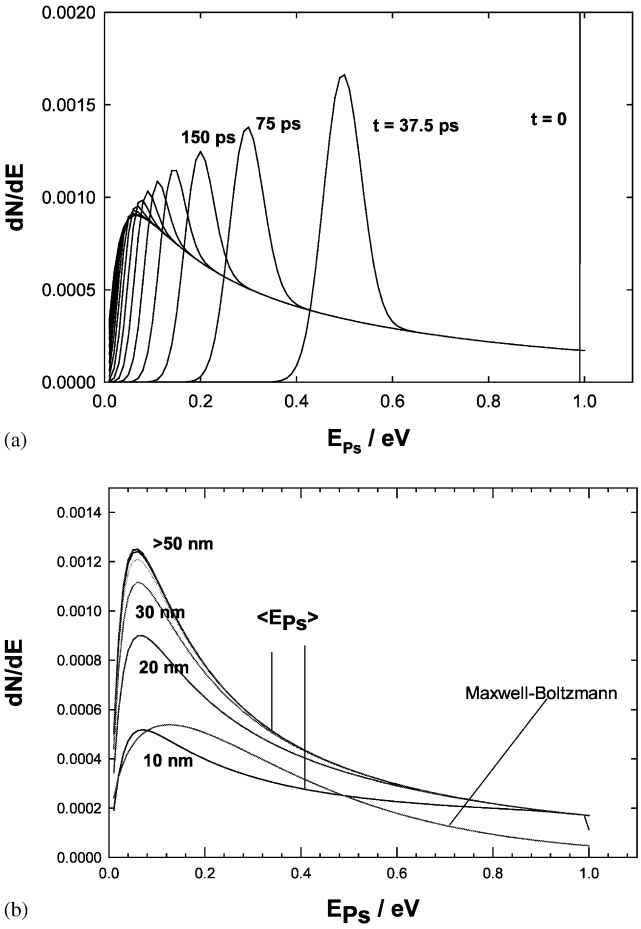

Fig. 4. (a) Calculated energy distributions during slowing down of p-Ps in mesoporous silica with pores of 5 nm and density 1 g cm^{-3} The Ps particles have an initial energy of 1 eV. The implantation of positrons is continuous with an energy of 3.5 keV at an average depth of 300 nm. The energy distribution is plotted at time intervals of 37.5 ps. After 500 ps a stationary state is attained. (b) Stationary energy distributions for different depths in the film. Average energies are indicated. A Maxwell–Boltzmann distribution is shown with similar average energy.

6. Conclusions and final remarks

Depth selective positron annihilation studies of low-k films show clearly that with increasing porosity of the films p-Ps created in the film is emerging from the film. The velocity distribution of the effusing Ps and the Ps remaining in the film can be determined. Cooling of the Ps is slow and is determined by interaction with the pore walls. The presence of o-Ps indicates that pores have grown beyond 4 nm size. Doppler broadening parameters and Ps fraction can be used to determine the

branching into all annihilation channels which depend on the porous structure of the film. The model presented here will in the future be used to perform fits of the branching ratios.

References

[1] M.P. Petkov, M.H. Weber, K.G. Rodbell, K.P. Lynn, S.A. Cohen, J. Appl. Phys. 86 (1999) 3104–3109.
[2] K.P. Rodbell, M.P. Petkov, M.H. Weber, K.G. Lynn, W. Volksen, R.D. Miller, Mater. Sci. Forum 363–365 (2000) 15–19.
[3] T. Gessmann, M.P. Petkov, M.H. Weber, K.G. Lynn, K.P. Rodbell, P. Asoka-Kumar, W. Stoeffl, R.H. Howell, Mater. Sci. Forum 363–365 (2000) 585–587.
[4] J. Sun, D.W. Gidley, T.L. Dull, W.E. Frieze, A.F. Yee, E.T. Ryan, S. Lin, J. Wetzel, J. Appl. Phys. 89 (2001) 5138–5144.
[5] R. Escobar Galindo, A. van Veen, S.W.H. Eijt, C.V. Falub, H. Schut, A.R. Balkenende, F.K. de Theije, Mater. Sc. Eng. B., this issue.
[6] A. van Veen, J. Trace Microprobe Techniques 8 (1&2) (1990) 1–29.
[7] A. van Veen, H. Schut, J. de Vries, R.A. Hakvoort, M.R. Ijpma, in: P.J. Schultz, G.R. Massoumi, P.J. Simpson (Eds.), Positron Beams for Solids and surfaces, AIP 218, 1990, pp. 171–196.
[8] A. van Veen, H. Schut, P.E. Mijnarends, in: P. Coleman (Ed.), Positron Beams and Their Applications, World Scientific Publishing, 2000 (Chapter 6).
[9] R.N. West, in: A. Dupasquier, A.P. Mills, Jr., (Eds.), Positron Spectroscopy of Solids, Proceedings of International School of Physics 'Enrico Fermi' Course CXXV' IOS Press, Amsterdam, 1995, 75–143.
[10] Y. Nagashima, M. Kakimoto, T. Hyodo, K. Fujiwara, A. Ichimura, T. Chang, J. Deng, T. Akahane, T. Chiba, K. Suzuki, B.T.A. McKee, A.T. Stewart, Phys. Rev. A 52 (1995) 258.